Amphiphilic core-shell nanoparticles with dimer fatty acid-based aliphatic polyester core and zwitterionic poly(sulfobetaine) shell for controlled delivery of curcumin

Daniel Gromadzki[1*], Virginia Tzankova[2], Magdalena Kondeva[2], Cvetelina Gorinova[2], Piotr Rychter[1], Marcin Libera[3], Georgi Momekov[2], Milan Marić[4], Denitsa Momekova[5*]

[1]*Institute of Polymers, Bulgarian Academy of Sciences, Acad. G. Bonchev 103A, 1113 Sofia, Bulgaria*

[2]*Department of Pharmacology, Pharmacotherapy and Toxicology, Faculty of Pharmacy, Medical University-Sofia, 2 Dunav Str., 1000 Sofia, Bulgaria*

[3]*Centre for Polymer and Carbon Materials of the Polish Academy of Sciences, M. Curie-Sklodowskiej 34, 41-819 Zabrze, Poland*

[4] *Department of Chemical Engineering, McGill University, 3610 University Street, Montreal, QC, Canada H3A 0C5*

[5]*Department of Pharmaceutical Technology and Biopharmaceutics, Faculty of Pharmacy, Medical University-Sofia, 2 Dunav Str., 1000 Sofia, Bulgaria*

[*]*Corressponding author: dgromadzki.pst@gmail.com (Dr. D. Gromadzki), dmomekova@yahoo.com (Prof. D. Momekova),*

Abstract

Multifunctional nanocarriers are gaining increasing research interest as polymeric platforms for targeted drug delivery in cancer therapy and diagnosis. In this work, preparation and characterization of surfactant-free polyester nanoparticles (NPs) from a bio-based poly (butylene sebacate-*co*-butylene dilinoleate)s, PBSE/PBDL, using nanoprecipitation, is reported. The polymeric nanoparticles (sizes narrowly distributed in a range less than 100 nm) were loaded with curcumin with an encapsulation efficiency of 98% and drug loading content of 5 -10% $wt_{drug}/wt_{polymer}$. The curcumin loaded nanoparticles were efficiently coated with a novel poly(sulfobetaine)-type zwitterionic polymer synthesized by Nitroxide Mediated Polymerization (NMP) and post-polymerization functionalization step. Free and curcumin formulated into non-coated and poly(sulfobetaine)-type zwitterionic polymer-coated nanoparticles were further investigated for cytotoxicity and antioxidant activity in a panel of human cell lines and rat liver microsomes respectively. Formulated into coated NPs curcumin has superior cytotoxic and antioxidant activity versus the free drug and curcumin incorporated in non-coated NPs. Additionally, cell viability experiments of non-loaded nanoparticles, both coated and non-coated, demonstrated that developed nanoparticles are non-toxic, making them potentially suitable candidates for systemic passive targeting in cancer therapy, namely for treatment of solid tumors exhibiting high tumor accumulation of NPs due to Enhanced Permeability and Retention (EPR) effect. Polyzwitterion coated nanoparticles exhibited slower drug release compared to the non-coated ones presumably due to the presence of the polymer shell around nanoparticles associated with a wider diffusion layer around the particles.

Keywords*: aliphatic polyesters, poly(sulfobetaine)s, biodegradable core-shell nanoparticles, drug delivery nanocarriers, cytotoxicity*

1. Introduction:

Amphiphilic diblock copolymer micelles have played an enormous role in drug and gene delivery[1,2,3]. The core-shell type of nanostructured drug delivery vehicle offers several advantages compared to the traditional treatment, as they enhance the drug bioavailability at the target site while minimizing the influence on the vital tissues and undesirable side effects[4,5]. Among the FDA-approved polymers, aliphatic polyesters such as poly(caprolactone) (PCL), polylactic acid (PLA) and poly(lactic-*co*-glycolic acid) (PLGA) have been extensively used for the manufacturing of drug delivery devices because of their good biodegradability, biocompatibility and drug release properties[6,7]. Poly(butylene sebacate) (PBS) is another interesting polyester that can be derived from renewable-based resources[8]. Recently, its copolymerization with different co-monomers led to novel materials exhibiting improved biodegradability and biocompatibility properties[9,10]. For example, long chain fatty acids (FA) are suitable monomers for the preparation of elastomeric biodegradable polymers since they are hydrophobic compounds and available commercially[11]. Herein, new biodegradable and biocompatible copolyesters composed of sebacic acid (SA), butanediol (BD) and dilinoleic acid (DLA) as building block monomers is proposed for the production of polymeric nanocarriers. The copolyester was synthesized by environmentally benign melt polycondensation using ‘‘green’’ monomers and characterized in detail by employing a variety of techniques. The nanoprecipitation (an interfacial deposition technique)[12] method was used for the manufacturing of spherical polyester nanoparticles with narrow size distribution, which formed a highly

hydrophobic polyester core ensuring efficient drug loading. Although the polyester nanoparticles were found fairly stable upon prolonged storage at room temperature, their application in true biophysiological conditions such as the blood plasma requires a protective shell. PEGylation, i.e. conjugation/coating of a polymer or nanocarrier with non-ionic oligomeric chains of poly(ethylene glycol) (PEG) has been a preferred route for introducing biocompatible and highly hydrophilic shells, which allows prolonged circulation times in a bloodstream without eliciting immunogenic responses[13,14]. Despite widespread application of PEG as a steric stabilizing agent of drug nanocarriers, it shows serious drawbacks such as susceptibility to oxidation degradation whereas PEGylation strongly inhibits cellular uptake and endosomal escape – the effect known as the "PEG dilemma"[15]. Recently, thermo-responsive brush-like copolymers comprising 2-(methoxyethoxy) ethyl methacrylate (MEO_2MA) and oligo(ethylene glycol) methacrylate (OEGMA) were proposed as a hydrophilic shell protecting a curcumin-loaded PLA core[16]. Overall, MEO_2MA-OEGMA copolymers are considered biocompatible[17] and similar coating materials are of increasing demand in the field of drug delivery. In the past few years, zwitterionic polymers attracted a lot of attention because they seem to share common traits with biomacromolecules like proteins and DNA[18,19]. Polyzwitterions including polysulfobetaines are well-known to exhibit very high bio- and haemocompatibility (their structure resembles the phosphorylcholine structure of cell membrane[20]) as well as ultra low fouling properties, making them desirable in various applications including nanocarrier formulations for active drug targeting[21,22,23,24,25]. From this perspective, the present paper will discuss synthesis of specially designed zwitterionic polysulfobetaine polymer based on 2-(dimethylamino)ethyl methacrylate, combining NMP and post-functionalization (betainisation with 1,3-butane sultone) chemistry, and successive grafting of (poly[4-((2-(methacryloyloxy)ethyl)dimethylammonio)butane-

1-sulfonate]) on the surface of drug loaded polyester nanoparticles through "arm first" EDC/NHS approach. The proposed coating strategy is expected to aid in efficient stabilization (stealth effect) of the hydrophobic core of the nanocarrier, preventing from its aggregation and non-specific protein adsorption from the blood plasma[26]. Furthermore, since the aqueous solution behavior of the zwitterionic polymer can be altered by temperature (lower-critical solution temperature (LCST) due to DMAEMA units and upper-critical solution temperature (UCST) due to zwitterionic units), pH, salt concentration and ionic strength, it provide an opportunity for active and passive drug targeting through EPR effect[27,28]. In 2014, Cao and co-workers reported carotene-loaded micelles comprised of amphiphilic core-shell nanostructures constructed of linear and star-shape poly(ε-caprolactone)-b-poly(N-(3-sulfopropyl)-N-methacryloxyethyl-N,N-diethylammoniumbetaine) (L/sPCL-b-PDEAS) with 4 and 6 arms synthesized with the combination of Ring Opening Polymerization (ROP) and Atom Transfer Radical Polymerization (ATRP)[29]. In vitro drug release experiment demonstrated that the release rate of carotene from the micelles was closely related to the arm numbers and drug loading content. Linear copolymer micelles exhibited the fastest release rate, 4-arm star shape copolymer micelles showed the lowest release rate. The micelles with higher drug loading content displayed lower release rate. Polyzwitterionic structures were scarcely investigated for drug delivery purposes and from this point of view it was interesting to use them in a self-assembly approach for constructing multifunctional macromolecular core-shell nanocarriers.

The model drug employed in this study is the natural polyphenol pigment curcumin. Curcumin (diferuloylmethane) is the main pharmacologically active principle of the spice turmeric, derived from the rhizomes of *Curcuma longa* L (Fam. Zingiberaceae).[30] A vast number of recent studies have shown that curcumin possessed a plethora of pharmacological effects, which include

antioxidant, anti-inflammatory, neuroprotective, chemopreventive and multimodal antineoplastic activities of possible clinical translation and value[31]. Despite its favorable pharmacological properties, there are some limitations for the development of curcumin as a potential therapeutic drug, including very low water solubility, low bioavailability *in vivo* and instability against UV light, which have greatly prevented the progression of this field beyond the preclinical level[32]. The curcumin plasma or tissue concentrations were reported to be either negligible or very low after oral administration in very high doses[33]. In addition to poor bioavailability, curcumin is unstable in aqueous solution at physiological pH and undergoes rapid biotransformation[34]. Considering the great potential of curcumin as a drug-candidate and the advantages of colloidal nanocarriers as a drug delivery platform, we detail the construction of amphiphilic core-shell nanoparticles containing curcumin with the aid of zwitterionic polymers and their resulting physico-chemical, antioxidant and antiproliferative properties were evaluated *in vitro*.

2. Experimental

2.1.Materials

Dimerized fatty acid (DFA) – hydrogenated dilinoleic acid (DLA), trade name Pripol 1009, (kindly provided by Croda, The Netherlands), 1,4-butanediol (BD, BASF), sebacic acid (SA, Aldrich Chemie), 2-(dimethylamino)ethyl methacrylate (DMAEMA, 98%, Sigma-Aldrich, Oakville, ON, Canada), acrylonitrile (AN, 99%, Sigma-Aldrich, Oakville, ON, Canada), *N*-(2-Methylpropyl)-*N*-(1-diethylphosphono-2,2-dimethylpropyl)-*O*-(2-carboxylprop-2-yl) hydroxylamine (BlocBuilder®,99%) was obtained from Arkema and used as received, *N*-hydroxysuccinimide (NHS, >97%, FlukaChemie), *N*-ethyl-*N′*-(3-diethylaminopropyl) carbodiimide hydrochloride (EDC, 99%, FlukaChemie), acetone (analytical grade, Fisher

Scientific, UK) and tetrahydrofuran (analytical grade, Fisher Scientific, UK), *N,N*-dimethylformamide (DMF). Magnesium-titanate organometallic complex (Mg–Ti) was prepared according to patented procedures. SpectraPor 7 dialysis membrane (MWCO 10000) Sigma-Aldrich (USA). 2-Thiobarbituric acid (TBA) and trichloroacetic acid (TCA) were obtained from Sigma Chemical Co. (St. Louis, MO USA). All other reagents were of analytical grade.

2.2. Methods

2.2.1.Synthesis of poly(butylene sebacate-co-butylene dilinoleate) PBSE/PBDL

Copolyesters were prepared by a typical melt polycondensation method as described elsewhere [10,11]. Briefly, the syntheses were carried out in a 1 dm^3 "pressure-vacuum" stainless steel reactor. The charge of the feed components was 2/3 of the reactor capacity (about 650 g). The esterification reaction between dimerized fatty acid (DFA), sebacic acid and 1,4-butanediol (1,4-BD) in the molar ratio 1:2.2 was carried out in the presence of magnesium-titanate organometallic complex (Mg–Ti) as a catalyst using intensive stirring and upon the programmed temperature rising from 100 °C to 200 °C with a heating rate of 1.5 °C/min. The reaction was finished when an acid value less than 2 mg $KOH \cdot g^{-1}$ had been reached. The polycondensation reaction was carried out at 245-250 °C, ~ 40 Pa and in the presence of the magnesium-titanate organometallic complex (Mg–Ti) catalyst. The reactor contents were extruded by means of compressed nitrogen. A copolyester with the composition PBSE/PBDL 50/50 wt% (PBSE refers to the hard crystallizable segment and PBDL refers to soft amorphous segment) was synthesized and used in this work. Number-average molar mass from size-exclusion chromatography (SEC) measured in chloroform and calibarated based on polystyrene standards was $\overline{M}_n$= 21300 g/mol, molar mass dispersity $Đ$ =1.99.

2.2.2. Synthesis of PBSE/PBDL nanoparticles

Polymeric NPs were prepared by interfacial polymer deposition following solvent displacement according to the methodology described elsewhere [8,10,11]. PBSE/PBDL copolyester was completely dissolved in acetone at 40 ºC and subsequently the organic phase was added drop-wise (EW- 74900-00, Cole-Parmer®) to deionized water under stirring. The solvent was evaporated and the suspension was concentrated under reduced pressure to yield the final concentration of 1 mg/mL. NPs were extensively dialyzed (Spectra/Por®6, 45×29 mm, MWCO 15 kD) against pure water before performing any further experiments. The prepared NPs were used immediately or stored at 4 ºC.

2.2.3. Synthesis of carboxyl-terminated poly(2-dimethylaminoethyl methacrylate-co-acrylonitrile) P(DMAEMA-co-AN) by nitroxide mediated polymerization

Nitroxide mediated copolymerization of DMAEMA in the presence of AN was performed according to procedures published elsewhere [9]. Briefly, DMAEMA (4.27 g, 0.027 mol), AN (0.0294 g, 5.54×10^{-4}mol), BlocBuilder® alkoxyamine (0.0656 g, 1.72×10^{-4}mol) and DMF (4.30 g, 0.058 mol) were added to a 50-mL, one-necked round-bottom glass flask and left stirring under nitrogen purge. After 10 min being sufficient for complete dissolution of initiator, the flask was connected to a condenser and inserted into a pre-heated (90 °C) oil bath. Reaction was carried out under nitrogen purge for 5.5 h. The resulting polymer was recovered by double precipitation in hexane, then decanted and dried overnight in vacuum at 50 °C. The target number-average molar mass ($\overline{M}_{n,target}$) at complete conversion, calculated by the mass of monomer relative to the moles of BlocBuilder® initiator, was set to 25 kg mol^{-1}. The yield was 53%. Number-average molar mass from SEC in THF based on poly(methyl methacrylate) calibration at 30 °C was $\overline{M}_n$ = 14500 g/mol, molar mass dispersity $Đ$ =1.70. The mole fraction of

AN units (1.1 mol %) was determined from ^{1}H NMR spectroscopy in $CDCl_3$ using integral of protons from methyl units ((C<u>*H*</u>$_3$)N-) attached to nitrogen atom of DMAEMA at 2.26 ppm to integral of protons from methine units (C<u>*H*</u>-) present in the main chain of AN. The copolymer composition was 99 mol% DMAEMA.

2.2.4. Betainisation of P(DMAEMA$_{99}$-co-AN$_1$)-SG1 polymer

Experimental conditions for the betainisation reaction were similar to a procedure first published by Armes and co-workers[35,36] and later adopted by others[37,38]. P(DMAEMA$_{99}$-*co*-AN$_1$) (1 g, 6.36 mmol of tertiary amine functional groups) was dissolved in THF (30 mL), and five-fold molar excess of 1,4-butane sultone (4.33 g, 0.032 mol) in THF (10 mL) was added dropwise to the stirring mixture at room temperature for 30 min. The reaction was carried out at room temperature and at 40 °C for 24 hours and it remained homogenous during the entire experiment. Afterwards, THF was removed by rotary evaporation under vacuum, dissolved in deionised H_2O, purified by extensive dialysis (3.5 kDa MWCO dialysis tubing) against deionised H_2O, and lyophilized. Two samples denoted as PZW1 and PZW2 with different substitution degree (D_S) were prepared, namely PZW1 (D_S = 60%) and PZW2 (D_S = 100%)

2.2.5. Coating of the NPs surface with poly(sulfobetaine) polymers

0.13 mM solution containing two-fold excess of carboxyl-terminated PZW polymer with respect to NPs concentration, 0.05 M *N*-hydroxysuccinimide and 0.5 mM *N*-ethyl-*N′*-(3-diethylaminopropyl) carbodiimide hydrochloride in MilliQ water was kept for 30 min at room temperature to activate the carboxylic groups and then transferred to the NP suspension (1 mg/mL). The coupling reaction was left reacting overnight and thereafter the reaction mixture was transferred for further purification by dialysis (Spectra/Por®6, 45×29 mm, MWCO 15 kD) for 24 hours.

2.2.6. Loading of PBSE/PBDL nanoparticles with curcumin

The nanoprecipitation technique was used to prepare the curcumin-encapsulated nanoparticles, PBSE/PBDL and drug were mixed in acetone (1 mg/mL) added drop wise to an aqueous solution rotating at 350 rpm. The resulting dispersion of nanoparticles was vacuum evaporated to eliminate the organic solvent and subjected to centrifugation at 10 000 rpm for 10 min to remove unloaded curcumin. The resulting clear to slightly opalescent yellow dispersions containing curcumin-loaded nanoparticles were collected and used for further experiments. The encapsulation efficacy (EE) was calculated as follows:

EE (%) = $(C_m/C_t) \times 100$, where C_m – micellar curcumin, C_t – total curcumin.

Drug loading capacity (DL) was calculated according to the equation:

$$DL = \frac{C_m}{C_p} \times 100$$

where C_m (mg) – entrapped curcumin and C_p – copolymer (mg)

The total amount of the hydrophobic model drug curcumin (CUR) loaded into the NPs was measured by UV-Vis spectrophotometer at λ = 427 nm after dissolving the NP in acetone.

2.2.7. Drug release

The *in vitro* curcumin release from bare PBSE/PBDL NPs and their poly(sulfobetaine)-type zwitterionic polymer-coated coated counterparts (PZW1 and PZW2) was evaluated by regular membrane dialysis at 37 °C against phosphate buffered saline solution (pH 7). 1 ml of the tested formulations was placed in dialysis membrane tubing (MWCO 10,000). The dialysis tubing was then placed in a temperature-controlled vessel, containing 100 ml buffer to which 10 % ethanol was added. At various time intervals, aliquots were taken from the acceptor medium and assayed for curcumin by UV-Vis spectroscopy at 427 nm. In order to establish whether the dialysis

membrane affects the diffusion of non-encapsulated curcumin, ethanol solution of pure drug at a concentration analogous to that in the nanoparticles was placed in an individual dialysis bag and dialyzed under the same conditions. The free curcumin was completely released form the bag for less than two hours.

2.2.8. Physicochemical characterization of the polymers and NPs:

Number-average molar mass ($\overline{M}_n$), mass-average molar mass ($\overline{M}_w$) and dispersity ($Đ_M = \overline{M}_w / \overline{M}_n$) were determined by SEC, which was calibrated relative to linear polystyrene standards with THF as the eluent at 35 ºC. A Waters Breeze SEC system was used at a mobile phase flow rate of 0.3 mL min^{-1} equipped with three Styragel HR columns (HR1 with a molecular weight measurement range of 10^2 to 5×10^3 g mol^{-1}, HR2 with a molecular weight measurement range of 5×10^2 to 2×10^4 g mol^{-1} and HR4 with a molecular weight measurement range of 5×10^3 to 6×10^5 g mol^{-1}) and a guard column. The SEC was equipped with a Waters 2487 UV detector and an RI 2410 differential refractive index (RI) detector. The molecular weight measurements were calibrated relative to poly(styrene) narrow molecular weight standards in THF at 35 °C.

^{1}H NMR was used to determine the copolymer composition. A 300 MHz Varian Gemini 2000 spectrometer was used for the ^{1}H NMR measurements. Samples were placed in 5 mm up NMR tubes using D_2O/750 mM NaCl as a solvent. After injecting and shimming, the samples were scanned 32 times.

The quasi-elastic light scattering (QELS) measurements were performed using a Malvern ZetaSizer (Nano-ZS). The instrument was equipped with a He-Ne laser operating at 633 nm and an avalanche photodiode detector. The solutions of NPs were not filtered before QELS measurement. The plastic cuvette was placed in the temperature-controlled measurement cell and equilibrated at the starting temperature for at least 30 min. The first-order intensity correlation

function, $g_1(t)$, was measured at a scattering angle of 173° using non-invasive back-scatter (NIBS) and analyzed by the method of cumulants to estimate the average decay rate, Γ, and the width of the decay, $\mu 2/\Gamma^2$.

$$g_1(t) = \exp[-\Gamma t + (\mu_2/2)t^2 - (\mu_3/3!)t^3 + ...] \quad (1)$$

The average decay rate Γ is given by:

$$\Gamma = Dq^2 \quad (2)$$

where D is the translational diffusion coefficient, and q is the magnitude of the scattering vector defined as:

$$q = \frac{4\pi n}{\lambda}\sin(\frac{\theta}{2}) \quad (3).$$

In Equation 3, n is the refractive index of the solvent, λ is the wavelength of the light in vacuum and θ is the scattering angle. In the limit of low concentrations, D can be approximated as the diffusion coefficient for spherical particles, D_o, which is related to the hydrodynamic diameter of the particles, D_h, by the Stokes-Einstein equation:

$$D_h = \frac{k_B T}{6\pi\eta D_0} \quad (4)$$

Where k_B is the Boltzman constant, T is temperature in Kelvin and η is the viscosity of the solvent. In the manuscript, mean hydrodynamic radius R_H was used as an average value from triplicate measurements. The ζ-potentials were calculated from the obtained electrophoretic mobility at 25 °C by the Smoluchowski equation [39]:

$$\xi = 4\pi\eta\upsilon/\varepsilon \quad (5)$$

where η is the solvent viscosity, υ is the electrophoretic mobility, and ε is the dielectric constant of the solvent.

2.2.3. Cryogenic Transmission Electron Microscopy (Cryo-TEM) visualization of nanoparticles

Cryogenic Transmission Electron Microscopy (cryo-TEM) images were obtained using a Tecnai F20 TWIN microscope (FEI Company, USA) equipped with field emission gun, operating at an acceleration voltage of 200 kV. Images were recorded on the Eagle 4k HS camera (FEI Company, USA) and processed with TIA software (FEI Company, USA). Specimen preparation was done by vitrification of the aqueous (HPLC grade water) solutions on grids with holey carbon film (Quantifoil R 2/2; Quantifoil Micro Tools GmbH, Germany). Prior to use, the grids were activated for 30 seconds in oxygen plasma using a Femto plasma cleaner (Diener Electronic, Germany). Cryo samples were prepared by applying a droplet (2.1 µL) of the solution to the grid, blotting with filter paper and immediate freezing in liquid ethane using a fully automated blotting device Vitrobot Mark IV (FEI Company, USA). After preparation, the vitrified specimens were kept under liquid nitrogen until they were inserted into a cryo-TEM-holder Gatan 626 (Gatan Inc., USA) and analyzed in the TEM at -178 °C. Images were processed using ImageJ software.

2.2.4. Cell lines and culture conditions.

The human tumor cell lines KG-1 (acute promyelocyte leukemia) and U-226 (multiple myeloma) were purchased from the German Collection of Microorganisms and Cell Cultures (DSMZ GmbH, Braunschweig, Germany), HepG2 (human hepatoma cells) originated from European collection of cell cultures - ECACC). The cells were grown routinely in a controlled environment - cell culture flasks with RPMI-1640 liquid medium supplemented with 10% fetal bovine

serum(FBS) and 2mML-glutamine, housed at 37°C in 5% CO_2 humidified atmosphere in an incubator 'BB 16-Function Line' Heraeus (Kendro, Hanau, Germany). The cells cultures were maintained in logarithmic growth phase by supplementation with fresh medium twice weekly. EJ cells were used before the seventh passage. Human hepatoma cells (HepG2) were kept in culture and expanded at 37 °C in a humidified atmosphere of 5% CO_2 in culture medium DMEM (Dulbecco's Modified Eagle's Medium, Lonza, Bazel, CH), supplemented with 20% fetal bovine serum (FBS) (Gibco BRL) at 10%, Penicillin/Streptomycin 100× (Euroclone, Devon, UK), Glutamax 100× (Invitrogen) and non-essential amino acids 100× (Invitrogen).

2.2.5. Cytotoxicity assessment (MTT-dye reduction assay)

The cellular viability and proliferation after exposure to the varying concentrations of PBSE/PBDL 50/50 and PBSE/PBDL/PZW nanoparticles was evaluated by using the standard MTT-dye reduction assay as described elsewhere [40] with slight modifications [41]. Exponentially growing cells were seeded in 96-well microplates at a density of $1x10^5$ cells/ml and were incubated at 37°C for 48 h. Afterwards, the cells were exposed to various concentrations (2, 3, 4, 5, 10 μg/ml) of free curcumin (as DMSO solution 1 mg/ml) or curcumin loaded PBSE/PBDL 50/50 and PBSE/PBDL/P(DMAEMA$_{100}$-*co*-AN$_1$) nanoparticles respectively for 48 h. For each concentration, 8 wells were used. After the incubation with the test compounds 10 μl MTT solution (10 mg/ml in PBS) aliquots were added to each well. The cells were further incubated for 4 h at 37 °C and the MTT-formazan crystals formed were dissolved by adding 100 μl/well 5% HCHO-acidified 2-propanol. The MTT formazan absorption was assessed using a microprocessor controlled microplate reader (LabeximLMR-1) at 580 nm. Cell

survival fractions were calculated as percentage of the untreated control. In addition, IC_{50} values were derived from the concentration-response curves (see below).

2.2.6. Animals and isolation of liver microsomes

Animals were purchased from the National Breeding Center, Sofia, Bulgaria. At least 7 days of acclimatization were allowed before the commencement of the study. The health was regularly monitored by a veterinary physician. The vivarium (certificate of registration of farm No. 0072/01.08.2007) was inspected by the Bulgarian Drug Agency in order to check the husbandry conditions (No. A-11-1081/03.11.2011). All performed procedures were approved by the Institutional Animal Care Committee and made according Ordinance No. 15/2006 for humaneness behavior to experimental animals.

Male Wistar rats (200–250 g) were fasted overnight and were sacrificed by cervical decapitation. Livers were thoroughly perfused with 1.15% KCl and homogenized with four volumes of ice-cold 0.1 M potassium phosphate buffer, pH = 7.4. The liver homogenate was centrifuged at 9 000 × g for 30 min at 4°C and the resulting postmitochondrial fraction (S9) was centrifuged at 105 000 × g for 60 min at 4°C. The microsomal pellets were re-suspended in 0.1 M potassium phosphate buffer, pH = 7.4, containing 20% glycerol. Aliquots of liver microsomes were stored at − 70°C until use [42]. Microsomal protein content was determined according to the method of Lowry et al. [43].

2.2.7. Nonenzymatic lipid peroxidation assay in liver microsomes

Rat liver microsomes (1 mg/ml protein) were preincubated with 0.025 mg/ml and 0.05 mg/ml free curcumin or with curcumin-loaded nanoparticles (concentrations equivalent to 2.5

μg/ml and 5.0 μg/ml curcumin, respectively) at 37 °C for 60 min, following incubation with 20 μM Fe^{2+} and 500 μM ascorbic acid at 37°C for 20 min [44].

The reaction mixture contained 0.15 M KCl/0.1 M potassium phosphate buffer, pH 7.4. Following incubation, the peroxidation was terminated by addition of 1 ml 25% (w/v) TCA and 1 ml 0.67% 2-TBAto the microsomes. The mixture was heated at 100 °C for 20 min. The absorbance was measured at 535 nm, and the amount of malondialdehyde (MDA) was calculated using a molar extinction coefficient of $1.56 \times 105/M^{-1}cm^{-1}$. The calculations were made by using the formula: MDA nmol/mg protein = E × 12.8 [45].

3. Results and discussion:

3.1. Synthesis and characterization of polymers

The synthetic strategies for bio-based polyesters comprised of PBSE/PBDL sequences as well as P(DMAEMA$_{99}$-*co*-AN$_1$)-SG1 polymer and its pH- and temperature responsive characteristics were already fully detailed elsewhere[8,9,10]. In this work a zwitterionic-type polymer was synthesized by post-polymerization modification (betainisation of tertiary amino groups with 1.4-butane sultone) of P(DMAEMA$_{99}$-*co*-AN$_1$)-SG1 yielding poly[4-((2-(methacryloyloxy)ethyl)dimethylammonio)butane-1-sulfonate]).

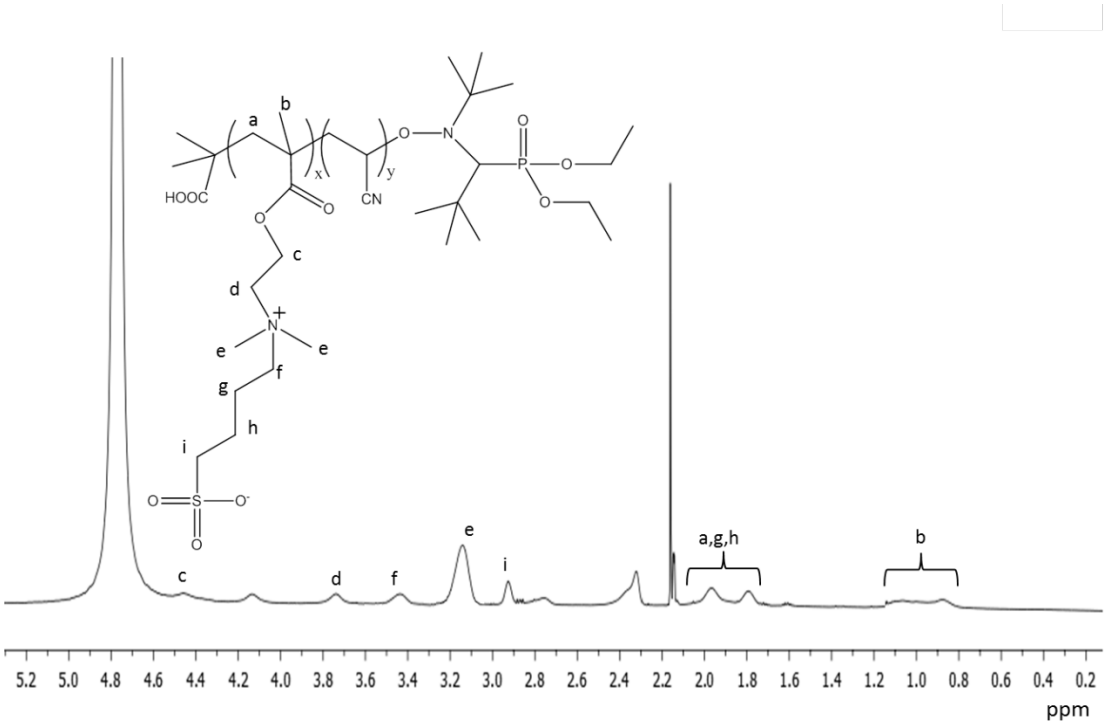

Figure 1.[1]HNMR (300 MHz) spectra of PZW1 measured in D_2O containing 750 mM NaCl.

Signals of PZW (Poly[4-((2-(methacryloyloxy)ethyl)dimethylammonio)butane-1-sulfonate]) ^{1}H NMR spectra were assigned as follows: δ/ppm = 4.45 (–OC*H*$_2$CH$_2$–), 3.73 (–OCH$_2$C*H*$_2$–), 3.44 (–N$^+$(CH$_3$)$_2$C*H*$_2$CH$_2$CH$_2$–), 3.14 (–N$^+$(C*H*$_3$)$_2$–), 2.91 (–C*H*$_2$SO$_3^-$), 1.96 (–N$^+$(CH$_3$)$_2$CH$_2$-C*H*$_2$CH$_2$– and backbone –CH$_2$–), 1.80 (–N$^+$(CH$_3$)$_2$CH$_2$CH$_2$C*H*$_2$–),1.00, 0.90 (backbone –CH$_3$). All the others signals (not described in text) are assigned to unreacted PDMAEMA. Detailed description of ^{1}HNMR spectra of P(DMAEMA$_{99}$-*co*-AN$_1$)-SG1 was presented in our previous work [8]. The degree of sulfobetainisation was calculated by integration of protons from methyl groups (*e*) to protons of methylene groups (*i*) adjacent to SO_3^- group according to formula:

$$D_S = \frac{e/6}{(e/6)+(i/2)} \times 100\% \quad (6)$$

Two copolymers with different substitution degree (D_S) were prepared, namely PZW1 (D_S = 60%) and PZW2 (D_S = 100%). Figure 1 represents a typical ^{1}HNMR spectrum of PZW1.

The solubility of novel PZW polymers in 0.5 wt. % solutions in deionized water (DW), phosphate buffer solutions (PBS) and NaCl solutions was investigated by QELS. The solutions were subjected to temperature ramp experiments from 20 °C to 55 °C. The hydrodynamic dimension of PZW polymers in DW was R_H = 173 nm at 20°C and it slightly decreased with increasing temperature up to 164 nm at 55°C. This result indicates a low hydration of PZW structures in DW, resulting in significant aggregation, which is typical of UCST-type polyzwitterions in aqueous salt-free solutions [46]. In PBS solutions PZW are almost completely dissolved with mean hydrodynamic radius around R_H = 5 nm, suggesting salt-responsive behavior of betainised PZW polymers. Finally, PZW polymer solutions containing NaCl exhibited similar behavior to PBS solutions. Thus, temperature did not play a significant role in altering the solution behavior of PZW polymers in PBS and NaCl solutions.

3.2. Synthesis, surface modification and characterization of multifunctional nanoparticles

Preparation of multifunctional nanoparticles comprising biodegradable core and dual-responsive shell was described in our previous paper[8]. The key difference of the current approach relies on using the biodegradable polyester to build up a hydrophobic core for loading of curcumin in the first step. Subsequently, the negatively charged NP surface is coated with polyzwitterionic polymers to render the particles highly biocompatible and stable in various biological media. The synthetic pathway is presented in Scheme 1.

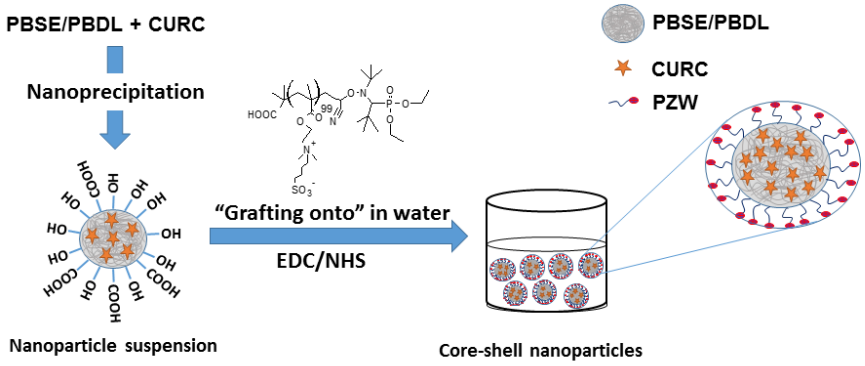

Scheme 1.Synthesis and drug loading of multifunctional NPs.

The nanoprecipitation protocol requires an organic solvent in which the PBSE/PBDL is fully soluble. The solvent must be also miscible in water and it must have a low boiling point to allow easy evaporation. Among the standard solvents, acetone was selected because it has proven to yield nanoparticles with appropriate sizes for controlled drug delivery (CDD) and very narrow particle size distributions[8]. The PBSE/PBDL is fully soluble in acetone as inferred from QELS measurements in our previous work [8,10]. The curcumin-loaded nanocarriers were prepared by means of nanoprecipitation. The PBSE/PBDL copolymer and curcumin are insoluble in water and the loaded nanoparticles are expected to undergo precipitation after the diffusion of acetone into the aqueous phase, with formation of well-defined nanoparticles with curcumin trapped in the hydrophobic core. The size, size distribution and the stability of the nanoparticles were investigated by QELS and the results are summarized in Table 1.

Table 1. Physico-chemical characteristics of the curcumin loaded PBSE/PBDL nanoparticles.

Entry	$c_{polymer}$ /mg mL^{-1}	R_H/nm	Dispersity	ζ/mV	$D_{H,\,av}$, (in range) Cryo-TEM (nm)

NP1	1.0	47.9±0.1	0.073±0.003	-28.0±0.2	68 (53-87)
NP2	5.0	307.0±0.6	0.065±0.006	-47.0±0.3	110 (102-118)
NP3	10.0	51.1±0.2	0.300±0.003	-23.0±0.2	73 (58-210)
NP4	15.0	49.1±0.4	0.065±0.002	-36.0±0.4	81 (61-220)

$c_{polymer}$ – polymer concentration; R_H – hydrodynamic radius; ζ- zeta potential; D_H – hydrodynamic diameter

The drug-loaded NPs were prepared using essentially the same nanoprecipitation procedure previously described except that in such a case, a known amount of CURC was dissolved in acetone along with the PBSE/PBDL copolyester. The drug loading capacity and encapsulation efficacy of the PBSE/PBDL NPs was investigated at 0.5:10, 1:10 and 2:10 $w_{drug}/w_{polymer}$ feeding ratio. It has been found that the encapsulation efficacy was above 98 % for the samples of 0.5-1:10 $w_{drug}/w_{polymer}$. The loading capacities of these samples were 5 and 10 % respectively. At the highest drug:polymer ratio, a lower encapsulation efficacy (EE=78 %) was observed. The drug loading capacity was 16 %, but the stability of this sample was compromised. The size of the CURC-free NPs was R_H = 60 nm (dispersity = 0.020 and ζ= - 49.9 mV) and it decreased upon loading with CURC to 47.9 nm to 51.1 nm as shown in Fig. 2. This NP contraction effect was previously observed when loading paclitaxel to nanoparticles and is related to a strong hydrophobic interaction of CURC with PBSE/PBDL polymer[11].

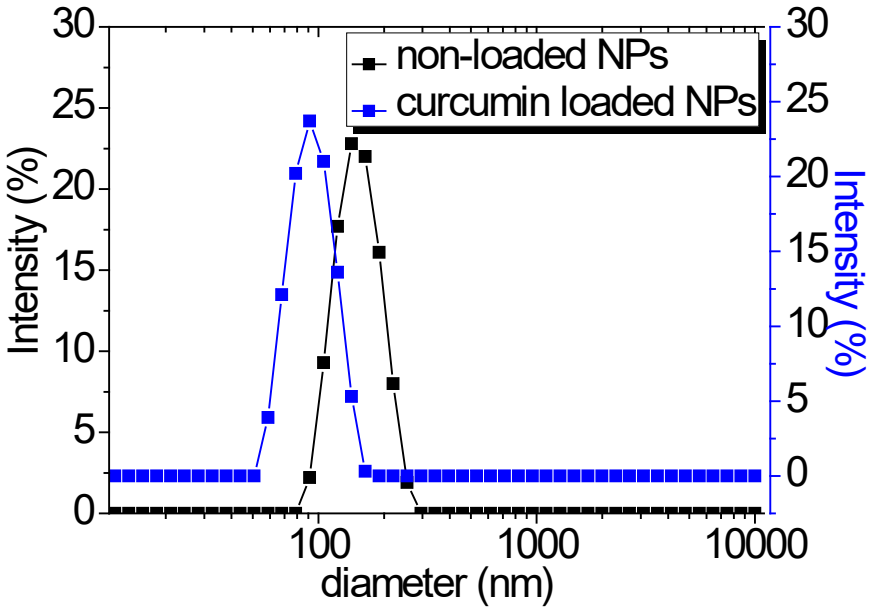

Fig. 2. Size distribution patterns of non-loaded and curcumin loaded NP1

In the current work, curcumin loaded NPs were chemically coated with PZW polymers through aqueous carbodiimide (EDC/NHS) coupling chemistry in order to confer the stability and improved release characteristics of these biodegradable nanocarriers. The size and NP dispersity was assessed by QELS. As indicated in Table 1, the size of CURC-loade NPs was around 50 nm with narrow size distribution and highly negative ζ. The chemical coating of NPs with betainised polymers led to an increase of the NP size up to R_H = 70 nm (dispersity = 0.113, ζ = 44.4 mV) and R_H = 90 nm (dispersity = 0.120, ζ = 44.4 mV) for PZW1 and PZW2 coated NPs, respectively. It is worth noting that upon coating of NPs with betainised polymers, the zeta potential turned from highly negative to highly positive, confirming efficiency of the applied coating strategy.

The spherical nanoparticles (both naked and CURC-loaded core-shell nanoparticles) are presented on the micrographs recorded using cryogenic transmission electron microscopy technique (cryo-TEM). Micrographs are presented on the Fig. 3.

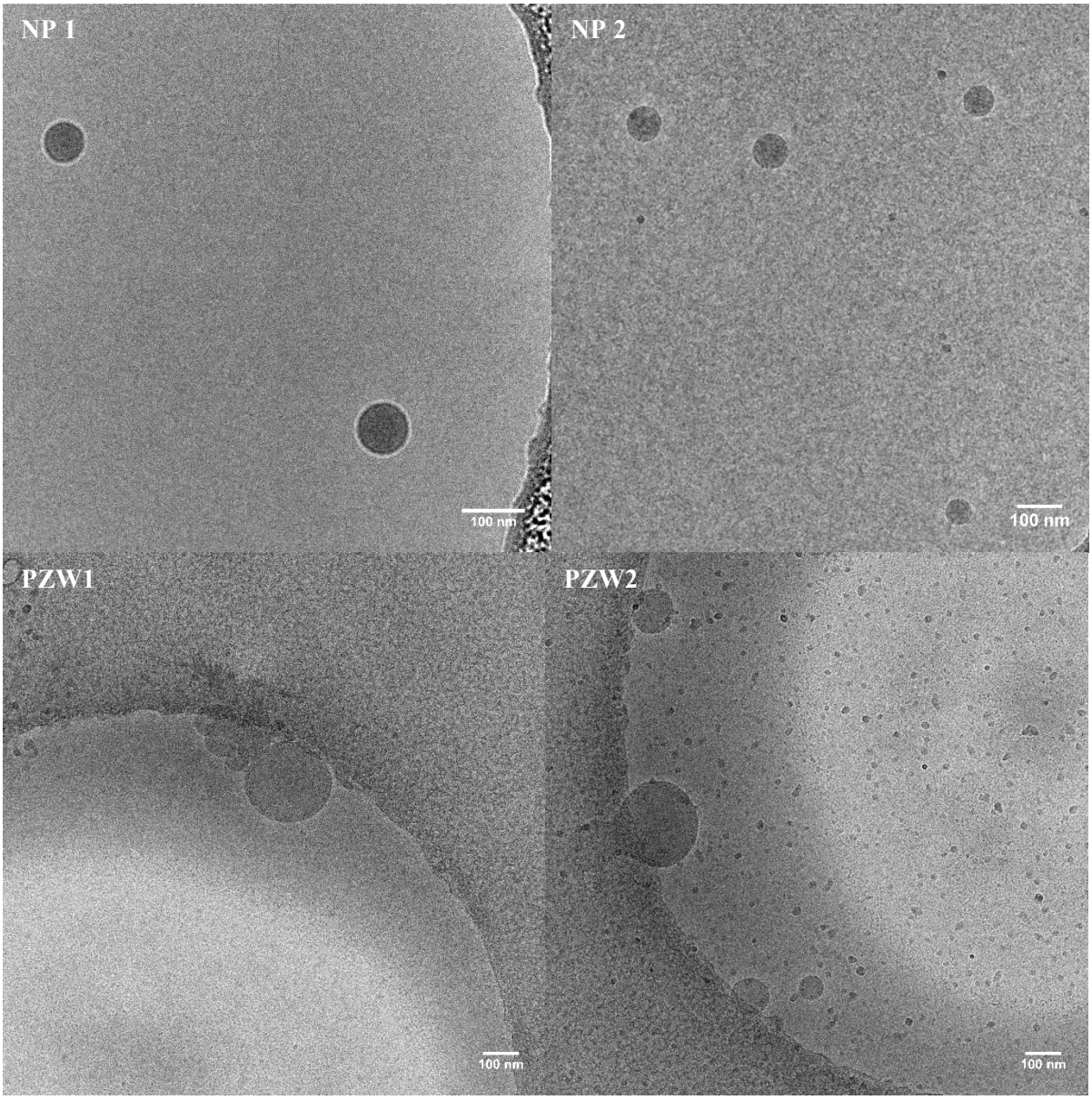

Fig. 3.Cryo-TEM micrographs of curcumin loaded non-coated nanoparticles (NP1, NP2) and PZW coated nanoparticles (PZW1, PZW2).

The vesicle nanostructure in water was preserved in its natural state by plunge freezing used during the cryo-preparation procedure. The thin film of amorphous ice, transparent to electrons, allowed for the observation of nanoparticles. The cryo-TEM micrographs were collected with a small negative defocus to improve phase contrast and at a low electron dose (less than 100e/Å^2/s) to prevent crystallization of the ice. The micrographs evidence vesicular structure of aggregated compounds.

Nanoparticles observed in cryo-TEM micrographs are of circular and rather regular shapes of unilamellar structure. The average diameters as well as size distribution of the vesicles calculated for 50 particles are given in Table 1.

Drug release

The release profile of CURC from PBSE/PBDL NPs and its surface modified counterparts was investigated by regular dialysis against PBS buffer (pH 7) at 37°C for a period of 24 hours. The release profiles of uncoated and PZW coated NP is shown in Figure 4.

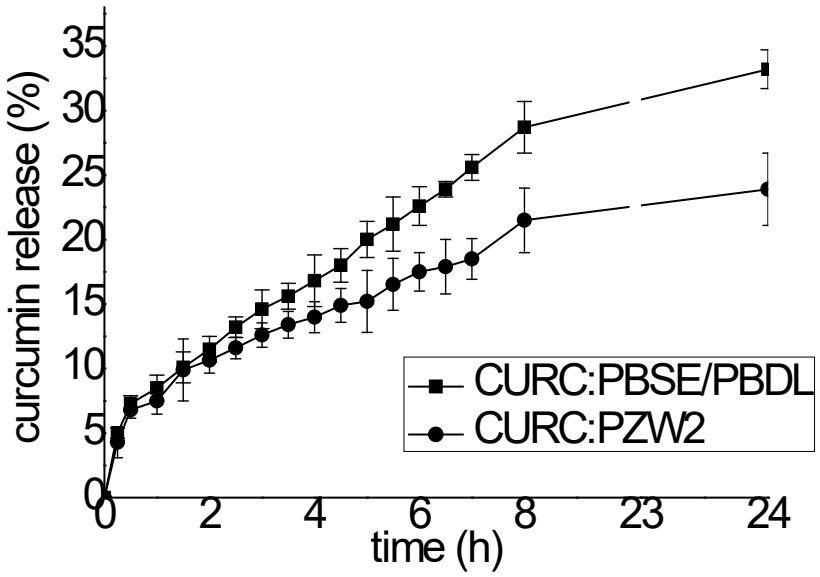

Fig. 4. Curcumin release profiles from uncoated CURC:PBSE/PBDL (■) and (●) PZW2 coated NPs at 37℃ in phosphate buffer (pH 7).

As evident from the data, the elaborated NPs are able to release the entrapped drug slowly (less that 32 % of incorporated CURC is released in 24 hours) and in a controlled manner. No initial burst release of CURC was observed, which indicate that the drug is most probably evenly distributed with the nanoparticles rather than absorbed on the surface. PZW2 nanoparticles exhibited lower drug release compared to the non-coated ones. This observation is most probably due to the presence of the polymer shell around PZW2 nanoparticles and associated with a wider diffusion layer around the particles.

Antiproliferative activity of curcumin-loaded PBSE/PBDLnanoparticles in vitro

A comparative evaluation of anti-proliferative activity of CURC applied as a DMSO solution or its nanoformulations (CURC-PBSE/PBDL, PZW1 and PZW2) was performed against two hematological human tumor cell lines, namely KG-1 (acute promyelocyte leukemia) and U-

226 (multiple myeloma) and one hepatoma cell line (HepG2). The cell lines were chosen as representatives of distinct types of white blood cells whereas HepG2 cells was used as a good model to study toxicity and xenobiotic biotransformation *in vitro*. HepG2 possess the activity of many enzymes involved in antioxidant defense mechanisms, as well as the phase I and II biotransformation enzymes, thus providing a suitable tool for studying antioxidant, anti-proliferative and cyto-protective effects of different compounds[47]. The concentration-effect response curves are depicted on Figure 5 and the corresponding equi-effective IC_{50} values are summarized in Table 2. In order to assess the alteration of the cytotoxicity of formulated *versus* free CURC the corresponding modulation indices were calculated as the ratios between the IC_{50} value of free drug and the IC_{50} value of the respective formulation.

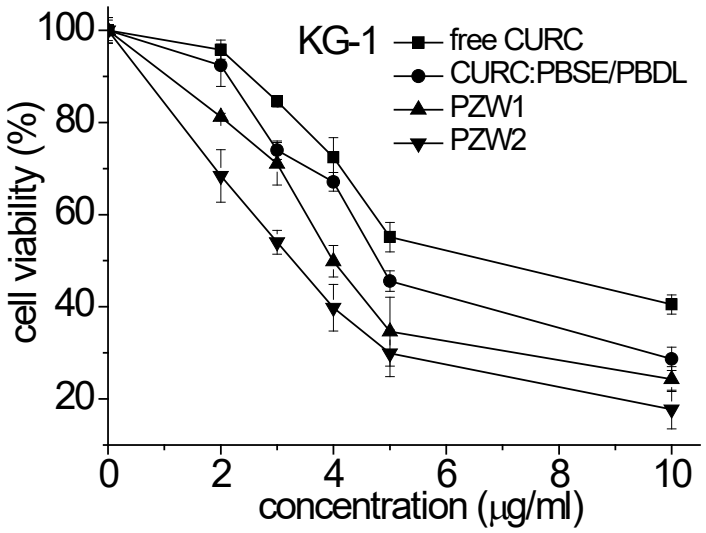

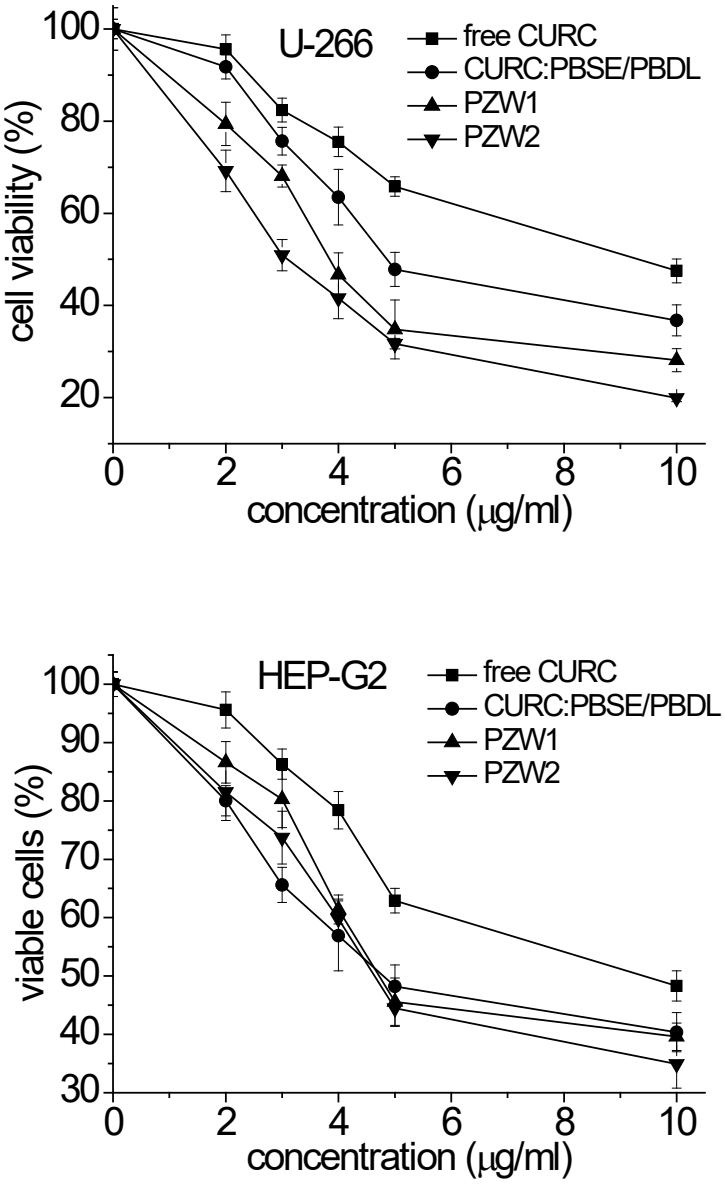

Figure 5.The growth inhibitory concentration-response curves as determined by the MTT-dye reduction assay after 48 hours continuous expousure. Each data point represents the arithmetic mean ± SD of 8 separate experiments.

Evident from the results, the CURC encapsulated within the PBSE/PBDL and its betainised counterparts showed superior cytotoxic activity compared to the free drug. Surface modification

of PBSE/PBDL NPs with poly(sulfobetaine)-type zwitterionic polymers is associated with further increase in antiproliferative activity. The concentration-response curves of those formulations were shifted to the lower concentrations and the corresponding IC_{50} values were lower compared to the effects of curcumin, applied as a DMSO-solution and non-coated counterparts. Thus, the CURC-PZW NPs have almost two fold lower IC_{50} values in all tumor models, as compared to the free CURC and near 30 % lower IC_{50}, as compared with curcumin incorporated into non-coated NPs. The assessment of the modulation indices shows that nanoparticles ascertained prominent augmentation of cytotoxicity of their cargo with modulation indices ranging *ca*. 1.4-3.1 (Table 2). Noteworthy, these trends were more noticeable for betainised nanoparticles (PZW1 and PZW2). The effect might be due to the improved cellular uptake of curcumin loaded in the nanoparticle drug delivery system. These findings well parallel previous studies that showed an increased cellular uptake of curcumin, when loaded into polymeric micelles in K-562 and U-226 cells *in vitro*[48]. To proved that the enhanced cytotoxicity of encapsulated curcumin vs. free agent is mainly due to the ability of the tested nanoparticles to internalize and deliver their cargo into the cytosol we south out to determine the cytotoxic potential of non-loaded NP1 nanoparticles and PZW1 free polymer on a panel of three human cell lines namely: KG-1 (acute promyelocyte leukemia), Hep-G2 (Human hepatoma cells) and a non-malignant HEK-293 (human embrional kidney cell). The concentrations of the tested non-loaded NPs were similar to the concentrations of curcumin-loaded NPs described above. The obtained concentration-response curves are presented on figure 6.

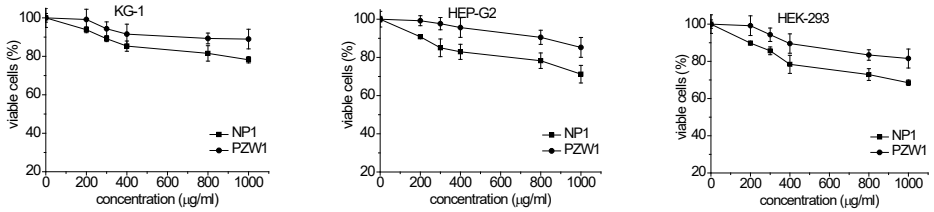

As evident from the results presented the unloaded nanoparticles as well as free PZW1 polymer are practically devoid from cytotoxic activity against the cell lines under investigation. Even at the highest tested concentrations (1000 μg/ml) the cell viability was only slightly affected over 70 % of treated cells retain their vitality as compared to the untreated control.

Thus, the results from our study suggests that CURC encapsulation into the proposed PBSE/PBDL nanoparticles could optimize its antiproliferative activity, possibly by improving

the drug transport and cellular uptake; however more studies are needed to elucidate the mechanism of this effect.

Table 2. Cytotoxicity of free curcumin and its formulations against human tumor cell lines after 48 h exposure

	KG-1 [a]		U-226 [b]		HepG-2[c]	
	IC_{50} (μg/ml)	MI [d]	IC_{50} (μg/ml)	MI [d]	IC_{50}(μg/ml)	MI [d]
Curcumin	6.68 ±2.31	-	9.3±2.77	-	9.37 ±3.7	
CUR-PBSE/PBDL	4.77± 1.44	1.4	4.87 ± 0.79	1.9	4.79±1.34	1.95
PZW1	3.98 ±0.84	1.8	3.84 ±1.02	2.4	4.71±0.79	1.99
PZW2	3.28±1.05	2.1	3.11 ± 0.59	3.1	4.65±1.54	2.02

[a]acutepromyelocyte leukemia; [b]multiple myeloma; [c]hepatoma cells [d]modulation index MI= IC_{50} (free curcumin)/ IC_{50} (curcumin formulation).

2. *Effect of curcumin and curcumin loaded PBSE/PBDL nanoparticles on nonenzymatic lipid peroxidation*

The effects of CURC and CURC-loaded nanoparticles on protection against Fe^{2+} - ascorbic acid (Fe^{2+}/AA) induced lipid peroxidation were studied in rat liver microsomes *in vitro*. Malondialdehide (MDA) was used as an index of the oxidative damage due to the lipid peroxidation (Fig. 2). The incubation of rat liver microsomes (1 mg/ml protein) in the presence of Fe^{2+}/AA resulted in induction of lipid peroxidation, as evidenced by the prominent increase in malondialdehide (MDA) production by 144% ($p<0.001$) *versus* the untreated control. When empty PBSE/PBDL nanoparticles (0.25 mg/ml and 0.5 mg/ml) were incubated with microsomes, MDA production was similar to that of untreated microsomes, thus showing that the PBSE/PBDL nanoparticles did not induce lipid peroxidation *per se* (data not shown).

Liver microsomes preincubated with free CURC (2.5 μg/ml and 5.0 μg/ml), following induction of oxidative stress with Fe^{2+}/AA, showed concentration-dependent inhibition of lipid peroxidation. Thus, the decrease in MDA production was 12% ($p<0.05$) and 41% ($p<0.001$) lower, respectively, *vs* control (Fe^{2+}/AA treated liver microsomes). The effect of CURC – loaded PBSE/PBDL nanoparticles on Fe^{2+}/AA induced lipid peroxidation was compared to those of free curcumin (at equivalent concentrations). CURC-loaded PBSE/PBDL nanoparticle formulation showed statistically significant effect on lipid peroxidation, lowering MDA production by 25% (at 2.5 μg/ml CURC) ($p<0.01$) and by 42% (5 μg/ml CURC) ($p<0.001$), *versus* Fe^{2+}/AA treated liver microsomes. It is interesting to note that in a dose, equivalent to 2.5 μg/ml CURC, the inhibitory effect on lipid peroxidation of uncoated NPs was inferior to that of free curcumin (Figure 6). This trend is more prominent for PZW1 and PZW2 coated nanoparticles. CURC:PZW1 (at 2.5 or 5μg/ml) were proven to decrease MDA production with 49 % and 53% respectively, while Cur:PZW2 nanoformulation inhibited MDA by 52 – 56 % vs. control. Similar to enhanced cytotoxicity the observed better antioxidant activity of formulated curcumin (especialy this curcumin loaded into PZW-modified NPs) vs. free drug could be explained with the optimized cellular internalization due to the positive charge of the coated nanoparticles.

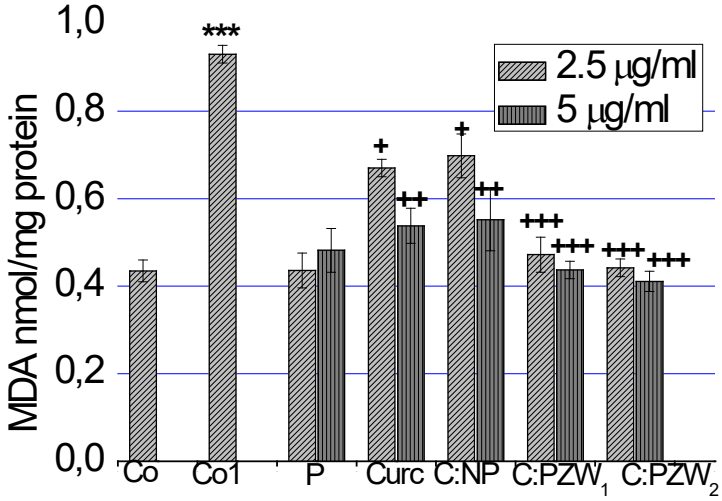

*Figure 6. Effect of CURC and CURC-loaded PBSE/PBDL nanoparticles on Fe^{2+}/AA -mediated lipid peroxidation in rat liver microsomes (mean ±S.E.M. n=6). The assay system and incubation conditions are described in Methods section. Values of ***p<0.001 (vs untreated control*

microsomes) and $^{+}p<0.05$, $^{++}$ $p<0.01$, $^{+++}p<0.001$ (vs Fe^{2+}/AA treated microsomes) were considered statistically significant.Co- untreated control, Co1-macrosomes with induced lipid peroxidation, P – non-loaded NPs,Curc-curcumin, C:NP-non-coated curcumin loaded NPs, C:PZW1 and C:PZW2 – curcumin loaded PZW1 and PZW2 coated NPs respectively.

Conclusions

A new generation of biocompatible core-shell NPs based on a bio-based polyester core and poly(sulfobetaine) shell was developed and investigated as a nanocarrier for delivery of CURC. The elaborated NPs are able to release the entrapped drug in a control manner (less that 32 % of incorporated CURC is released in 24 hours) with absence of initial burst release of CURC. PZW2 nanoparticles have shown slower drug release as compared to the non-coated ones. The results from our study showed that CURC loading in PBSE/PBDL nanoparticles increased its antiproliferative activity against the all tested mallignanthuman cell lines *in vitro*. Furthermore, the incorporation of CURC in PBSE/PBDL and especially in their betainisated PZW counterparts improved the inhibitory effects on Fe^{2+}/AA–induced lipid peroxidation compared to the free curcumin.

Acknowledgement

This work was financed by the European Commission's FP7-POLINNOVA (Grant 316086) project. Polyester synthesis was performed with assistance of Dr. A. Kozlowska from The West Pomeranian University of Technology in Szczecin, Poland. We are grateful to Prof. N. S. Koseva from the Bulgarian Academy of Sciences for providing 1.4-butane sultone, helpful discussions on polyzwitterion structures and support of this work.

[1] K. Kataoka, A. Harada and Y. Nagasaki, *Adv. Drug Delivery Rev.*, 47, 113, **2001**.
[2] V. P. Torchilin, *Pharm. Res.,* 24, 1, **2007**.
[3]D.E. Discher, A. Eisenberg, *Science*, 9;297(5583):967-73, **2002**.
[4]D. Peer, J. M. Karp, S. Hong, O. C. Farokhzad, R. Margalit, R. Langer, Nanocarriers as an emerging platform for cancer therapy, *Nature Nanotechnology* 2, 751 – 760, **2007**.
[5]M.-C. Jones, J.-C.Leroux, Polymeric micelles – a new generation of colloidal drug carriers, Eur. J. Pharm. Biopharm. 48, 101–111, **1999**.
[6]J. M. Anderson and M. S. Shive, Adv. *Drug Delivery Rev.,* 28, 5– 24, **1997**.
[7]S. Slomkowski, S. Penczek, A. Duda, *Polym. Adv. Technol.*, 25: 436–447, **2014**.
[8]Y. Tokiwa, B. P. Calabia, C. U. Ugwu, S. Aiba, *Int. J. Mol. Sci.* 10, 3722-3742, **2009**.
[9]D. Gromadzki, P. Rychter, M. Uchman, D. Momekova, A. Marcinkowski, *et. al*. *Macromol. Chem. Phys.*, 216, 2287-2301, **2015**.
[10] A. Kozlowska, D. Gromadzki, M. El Fray and P. Stepanek, *Fib. Text. East Eur.,*71, 85–88, **2008**.
[11] A. Jäger., D. Gromadzki, E. Jäger, F.C. Giacomelli, A. Kozlowska, L. Kobera, J. Brus, B. Říhová, M. El Fray, K. Ulbrich, P. Štěpánek, *Soft Matter*, 8, 4343, **2012**.
[12] H. Fessi, F. Puisieux, J.Ph. Devissaguet, N. Ammoury, S. Benita, International Journal of Pharmaceutics, 55, R1-R4, **1989**.
[13] H. Otsuka, Y. Nagasaki, K. Kataoka, PEGylated nanoparticles for biological and pharmaceutical application. *Adv Drug Deliv Rev* 55, 403–419, **2003**.
[14]D. Gromadzki, A. Jigounov, P. Stepanek, R. Makuska, *Eur. Polym. J.*,46, 804–813, **2010**.
[15] H. Hatekeyama, H. Akita, H. Harashima. *Adv Drug DelivRev* ,63, 152-160, **2011**.
[16] Y. Hu, V. Darcos, S. Monge, S. Li. *International Journal of Pharmaceutics*, 491, 1-2, 152-161, **2015**.
[17] J.F. Lutz, *Adv. Mater.*, 23, 2237–2243, **2011**.
[18]Dobrynin, A.V.; Rubinstein, M. *Prog.Polym.Sci.*,30,1049, **2005**.
[19] P.G. Higgs, P.G., J.F. Joanny, *J.Chem.Phys.*, 94,1543, **1991**.
[20] R. Lalani, L. Liu, *Biomacromolecules*, 13, 1853, **2012**.
[21]Y. Chang, W. Yandi, W.-Y.Chen, Y.-J.Shih, C.-C.Yang, Y. Chang, Q.-D. Ling and A. Higuchi, *Biomacromolecules*, 11, 1101–1110, **2010**.
[22]A. J. Keefe and S. Jiang, *Nat. Chem.*, 4, 59-63, **2012**.
[23] P. Mary, D. D. Bendejacq, M. P. Labeau, P. Dupuis, *J. Phys. Chem.* B, 111, 7767-7777, **2007**.
[24]Z. Zhang, J. A. Finlay, L. Wang, Y. Gao, J. A. Callow, M. E. Callow, S. Jiang, *Langmuir*, *25* (23), 13516–13521, **2009**.
[25]XiaoxiongXiea, YuhaoMaa, Lei Huanga, MengtanCai, Yuanwei Chena, Xianglin Luo, Colloids and Surfaces A: Physicochem. Eng. Aspects 468, 31–39, **2015**.
[26] A.V. Kabanov, E.V. Batrakova, N.S. Melik-Nubarov, N.A. Fedoseev, T.Y. Dorodnich, V.Y. Alakhov, V.P. Chekhonin, I.R. Nazarova, V.A. Kabanov, new class of drug carriers: micelles of poly(oxyethylene)-poly(oxypropylene) block copolymers as microcontainers for drug targeting form blood in brain, *J. Control. Rel.* 22, 141-158, **1992**.
[27] Maeda, H., Macromolecular therapeutics in cancer treatment: The EPR effect and beyond. *J Control. Rel.*, 164, (2), 138-144, **2012**.
[28]F. Alexis, E. Pridgen, L. K. Molnar, O. C. Farokhzad, *Mol. Pharmaceutics*, **2008**, *5* (4), pp 505–515.
[29] J. Cao, A. Lu, C. Li, M. Cai, Y. Chen, S. Li, X. Luo, *Colloids and surfaces B: Biointerfaces*, 112C:35-41., **2013**.
[30] (a) Shehzad A, Wahid F, Lee YS. *Arch Pharm (Weinheim).* **2010**, 343(9):489-99. (b) Singh S, Khar A., *Anticancer Agents Med Chem.* 6(3):259-70, **2006**.

[31] (a) O'Sullivan-Coyne, G.; O'Sullivan, G.C.; O'Donovan, T.R.; Piwocka, K.; McKenna, S.L.Curcumin induces apoptosis-independent death in oesophageal cancer cells. *Br. J. Cancer*,101, 1585–1595, **2009**. (b) Chuengsamarn, S.; Rattanamongkolgul, S.; Luechapudiporn, R.; Phisalaphong, C.; Jirawatnotai, S. Curcumin extract for prevention of type 2 diabetes. *Diabetes Care*, 35, 2121–2127, **2012**. (c) Thakare, V.N.; Osama, M.M.; Naik, S.R. Therapeutic potential of curcumin in experimentally induced allergic rhinitis in guinea pigs. *Int. Immunopharmacol*., 17, 18–25, **2013**. (d) Huang, G.; Xu, Z.; Huang, Y.; Duan, X.; Gong, W.; Zhang, Y.; Fan, J.; He, F. Curcumin protects against collagen-induced arthritis via suppression of BAFF production. J. Clin. Immunol., 3, 550–557, **2013**. (e) Kusuma, A.; Colpitts, C.C.; Schang, L.M.; Rachmawati, H.; Frentzen, A.; Pfaender, S.; Behrendt, P.;Brown, R.J.P.; Bankwitz, D.; Steinmann, J.; et al. Turmeric Curcumin Inhibits Entry of All Hepatitis C Virus Genotypes into Human Liver Cells. *J. Hepatol.* 58, S473–S473, **2013**.

[32] (a) Anand, P.; Kunnumakkara, A.B.; Newman, R.A.; Aggarwal, B.B. Bioavailability of curcumin: Problems and promises. *Mol. Pharm*., 4, 807–818, **2007**. (b) Pan, M.H.; Huang, T.M.; Lin, J.K. Biotransformation of curcumin through reduction and glucuronidation in micse. *Drug Metab. Dispos*., 27, 486–494, **1999**.

[33] (a) Dhillon, N.; Aggarwal, B.B.; Newman, R.A.; Wolff, R.A.; Kunnumakkara, A.B.; Abbruzzese, J.L.;Ng, C.S.; Badmaev, V.; Kurzrock, R. Phase II trial of curcumin in patients with advanced pancreatic cancer. *Clin. Cancer Res*., 14, 4491–4499, **2008**. (b) Sharma, R.A.; Euden, S.A.; Platton, S.L.; Cooke, D.N.; Shafayat, A.; Hewitt, H.R.; Marczylo, T.H.; Morgan, B.; Hemingway, D.; Plummer, S.M.; et al. Phase I clinical trial of oral curcumin: Biomarkers of systemic activity and compliance. *Clin. Cancer Res*., 10, 6847–6854, **2004**. (c) Cheng, A.L.; Hsu, C.H.; Lin, J.K.; Hsu, M.M.; Ho, Y.F.; Shen, T.S.; Ko, J.Y.; Lin, J.T.; Lin, B.R.; Ming-Shiang, W.; et al. Phase I Clinical Trial of Curcumin, a Chemopreventive Agent, in Patients with High-Risk or Pre-Malignant Lesions. Anticancer Res., 21, 2895–2900, **2001**.

[34]Lin, J.K.; Pan, M.H.; Lin-Shiau, S.Y. Recent studies on the biofunctions and biotransformations of curcumin. BioFactors 13, 153–158, **2000**.

[35] A. B. Lowe, S. P. Armes and N. C. Billingham, *Chem. Commun.,*1997, 671-672.

[36] V. Bütün, C. E. Bennett, M. Vamvakaki, A. B. Lowe, N. C. Billingham, S. P. Armes, *J. Mater. Chem.*, 7(9), 1693–1695, **1997**.

[37] I. Javakhishvili, K. Jankova and S. Hvilsted, *Polym. Chem.*, 2013, 4, 662.

[38] H. Willcock, A. Lu, C. F. Hansell, E. Chapman, I. R. Collinsb and Rachel K. O'Reilly, *Polym. Chem.,* 5, 1023, **2014**.

[39] M. Smoluchowski. Zur kinetischen Theorie der Brownschen Molekularbewegung und der Suspensionen. *Annalen der Physik*. **326** (14): 756–780, 1906.

[40] T. Mosmann. Rapid colorimetric assay for cellular growth and survival: application to proliferation and cytotoxicity assays *J Immunol Methods.*16, 65 (1-2): 55-63, **1983**.

[41] S.M. Konstantinov, H. Eibl, M.R. Berger, BCR-ABL influences the antileukaemic efficacy of alkylphosphocholines. - *Br. J. Haematol*., 107, 365-380, **1999**.

[42]Simeonova RL, Vitcheva VB, Kondeva-Burdina MS, Krasteva IN, Nikolov SD, Mitcheva MK. Effect of purified saponin mixture from Astragaluscorniculatus on enzyme- and non-enzyme-induced lipid peroxidation in liver microsomes from spontaneously hypertensive rats and normotensive rats.Phytomedicine 2010;17:346-9.

[43] Lowry OH, Rosebrough NJ, Farr AL, Randall RJ. Protein measurement with the Folin phenol reagent.J Biol Chem 1951;193:265-75.

[44]Kim HJ, Chun YJ, Park JD, Kim SI, Roh JK, Jeong TC. Protection of rat liver microsomes against carbon tetrachloride-induced lipid peroxidation by red ginseng saponin through cytochrome P450 inhibition. Planta Med 1997;63:415-8.

[45]Deby C, Goutier R. New perspectives on the biochemistry of superoxide anion and the efficiency of superoxide dismutases.BiochemPharmacol 1990;39:399-405

[46] Chen, S., Li, L., Zhao, Ch., Zheng, J. Surface hydration: Principles and applications toward low-fouling/nonfouling biomaterials. Polymer 51; 23; 5283-5293, 2010.

[47]Mersch-Sundermann, V., Knasmüller, S., Wu, S., Darroudi, F., Kassie,F.Use of a human-derived liver cell line for the detection of cytoprotective, antigenotoxic and cogenotoxic agents. Toxicology 2004; 198 (1–3), 329–340.

[48]Yoncheva K, Kamenova K, Perperieva T, Hadjimitova V, Donchev P, Kaloyanov K, Konstantinov S, Kondeva-Burdina M, Tzankova V, Petrov P. Cationic triblock copolymer micelles enhance antioxidant activity, intracellular uptake and cytotoxicity of curcumin. Int J Pharm. 2015 Jul 25; 490(1-2):298-307.